PROCEEDINGS, 49th Workshop on Geothermal Reservoir Engineering
Stanford University, Stanford, California, February 12-14, 2024
SGP-TR-227

Updates on the Development of Chloride-based Wireline Tool for Measuring Feed Zone Inflow in Enhanced Geothermal Systems (EGS) Wells

Sarah Sausan[1], Marshall Hartung[1], Jiann-cherng Su[2], Melanie B. Schneider[2], Andrew A. Wright[2], and Roland N. Horne[1]

[1]Dept. of Energy Science and Engineering, Stanford University

[2]Sandia National Laboratories

sausan@stanford.edu, hartung1@stanford.edu, jsu@sandia.gov, mbschne@sandia.gov, aawrigh@sandia.gov, horne@stanford.edu

Keywords: chloride concentration, fracture inflows, Utah FORGE, EGS, chloride, single phase

ABSTRACT

This paper presents the ongoing development of a chloride-based wireline tool designed to detect and quantify inflows from feed zones in geothermal wells. The tool aims to characterize stimulation events in EGS wells at Utah FORGE (Frontier Observatory for Research in Geothermal Energy) and other EGS sites. Successful development of the chloride tool would greatly improve production monitoring of the fractures and enable proactive prescription of additional stimulations over the life of the field, thus helping to improve EGS commercial feasibility.

The recent developments of the chloride tool focused on the field scale in preparation for the field test at the Utah FORGE site. A high-temperature Chemical Buffer Amplifier (CBA) board was designed to operate at 260°C, and an alternative system microcontroller from Analog Devices is being explored for data transmission at 200°C. The tool assembly includes a PTS sensor package, a wire guide component, and an electronics housing for data transmission through a 7-conductor feedthrough. Numerical simulations at the field scale were conducted under downhole conditions (225°C and 5000 psia) and showed no significant change in fluid flow behavior compared to laboratory conditions. Further simulations focused on the design of the field-scale tool housing. Simulations assessed ten different positions relative to the feed zone height. The simulations suggested that the best signal recordings occurred at the beginning of the tool's Run in Hole (RIH) motion when the lower part of the housing met the feed zone.

Several improvements were also made to the laboratory apparatus, which involved addressing the electrical noise issue affecting the voltage readings of the laboratory-scale chloride tool. Changing the reservoir pump from AC to DC and wrapping various electronic sources with Faraday fabric have greatly dampened the interference noise in the voltage readings. Additionally, the routing mechanism of the tool running system was reconfigured to improve the tool movements and enhance deployment control.

Sandia National Laboratory is managed and operated by NTESS under DOE NNSA contract DE-NA0003525.

1. INTRODUCTION

Enhanced Geothermal Systems (EGS) use artificial fractures to increase fluid extraction in less permeable geothermal reservoirs (Huenges, 2016). Artificial fractures are created through hydraulic stimulation and may close over time, reducing the productivity of the EGS wells (Fei et al., 2023). By monitoring the productivity of artificial fractures, operators can prescribe mitigation techniques such as restimulation. Timely interventions can help to keep the fractures open and flowing throughout the geothermal plant's lifetime, which typically lasts between 30 and 50 years (Sullivan et al., 2010).

The pressure-temperature-spinner (PTS) tool is commonly used to measure inflow rates from feed zones, with the spinner part determining the flow rate (Sisler et al., 2015). PTS tools show limitations in wells with low fluid velocity, low enthalpy, and large diameters (Acuña and Arcedera, 2005). The study found that there was an overestimation of the inflow rate in the vertical section compared to the nonvertical section of the well. Furthermore, changes in hole diameter outside of slotted liners can influence spinner rotation, which could be misinterpreted as an actual change in flow rate.

A geochemistry-based alternative to the PTS tool is being developed by the Stanford Geothermal Program and Sandia National Laboratory as part of the Utah Frontier Observatory for Research in Geothermal Energy (FORGE) project. This tool uses an ion-selective electrode to measure chloride concentration via electrical voltage. The reference electrode serves as the reference potential for the pair (Figure 1). Different chloride concentration readings around the feed zone can be used to calculate the feed zone inflow rate. In this work, this tool is referred to as the "chloride tool". A major advantage of the chloride tool is that it does not require knowledge of the hole diameter, which is a limitation of a spinner tool.

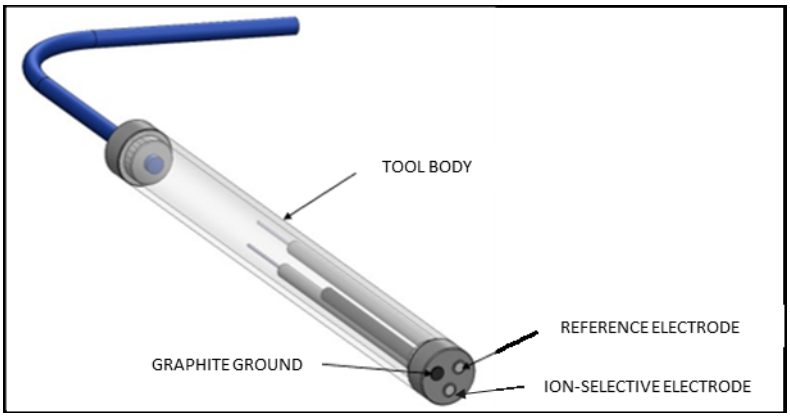

Figure 1: Lab-scale chloride tool schematics, taken from Sausan et al. (2023).

This study expanded on a previous investigation by Gao et al. (2017), which used a chloride tool prototype that was developed by Sandia National Laboratory (Cieslewski et al., 2016; Corbin et al., 2017). In the preliminary study, the team used measurements from the ion-selective electrode to estimate the enthalpy of the feed zone. They targeted chloride concentrations because chloride is consistently present in the liquid phase of geothermal reservoirs. (Sausan, 2023).

Building upon that previous research, this study aims to develop a field-deployable version of the chloride tool to be used at the Utah FORGE project, which features EGS wells with single-phase fluid and multiple feed zones. This study focuses on estimating the feed zone inflow rate, specifically in single-phase flow conditions, rather than enthalpy. The ultimate goal is to leverage insights from the Utah FORGE field trial for broader applications across various EGS sites.

More importantly, this study is exploring a wider role of geochemistry, indicated by the chloride species concentration change, in determining fluid flow patterns in geothermal wells. Typically, the practical application of geochemistry in the geothermal industry revolves around estimating enthalpy or using tracer studies. However, this wider use of geochemistry could enhance our comprehension of the behavior of geothermal wells and fields.

This study employed a multifaceted approach, integrating analytical methods, numerical simulations, laboratory experiments, data science techniques, and field trials. Previously reported progress can be found at Sausan et al. (2021, 2023) and Judawisastra et al. (2022, 2023). This paper highlights the latest progress involving field-scale tool fabrication and testing, laboratory setup improvements, and numerical simulations involving the field-scale tool housing and at Utah FORGE temperature and pressure operating conditions. Additionally, the deployment plan is given in preparation for the upcoming field deployment at the Utah FORGE site.

2. UPDATES ON TOOL DEVELOPMENT AND ASSEMBLY

2.1 Tool Development and Assembly

2.1.1 High Temperature Logging Tool

Sandia modified an existing high-temperature (HT) logging tool to deploy the chemical sensors into the Utah FORGE well. The tool uses a previously deployed and tested capability to capture and transmit the data from the chemical sensors to the surface. The tool uses a Honeywell HT HT83C51 microcontroller in parallel with a Sandia custom high-temperature Application-specific Integrated Circuit (ASIC). This tool was developed to capture pressure, temperature, and flow using Mitco's pressure, temperature, spinner module (PTS). The tool uses Frequency Shift Keying (FSK) and a multiconductor wireline to transmit data to the surface. Figure 2 shows the electronics for the logging tool placed next to Mitco's PTS module.

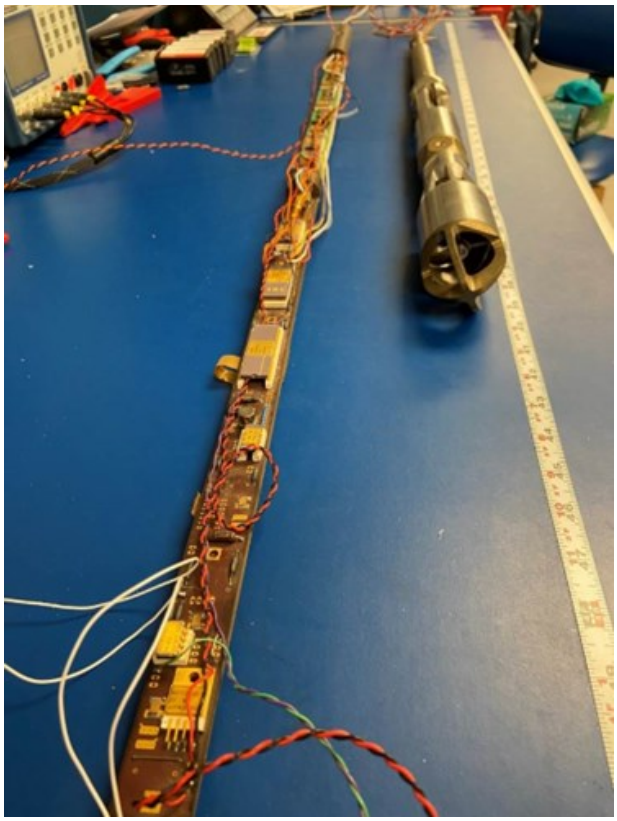

Figure 2: Sandia's custom high-temperature logging tool with Honeywell's microcontroller and Sandia's custom Application-specific Integrated Circuit or ASIC (left) next to Mitco's PTS module (right).

A new high-temperature expansion board was developed to accommodate the additional signal inputs for the chemical sensors. Figure 3 shows the high-temperature Chemical Buffer Amplifier (CBA) board, which was designed to take the high-impedance signal from the sensor to a low impedance while amplifying the signal. Using Sandia's high-temperature tool, the signal is digitized with the onboard Analog-to-digital Converter (ADC). The components of this system are rated to operate at 260 ˚C. With the populated CBA, the system will be tested with the chemical sensors while being heated in the oven to confirm the proper operation of the board. A housing extension was designed and fabricated to incorporate this new board with the high-temperature logging tool.

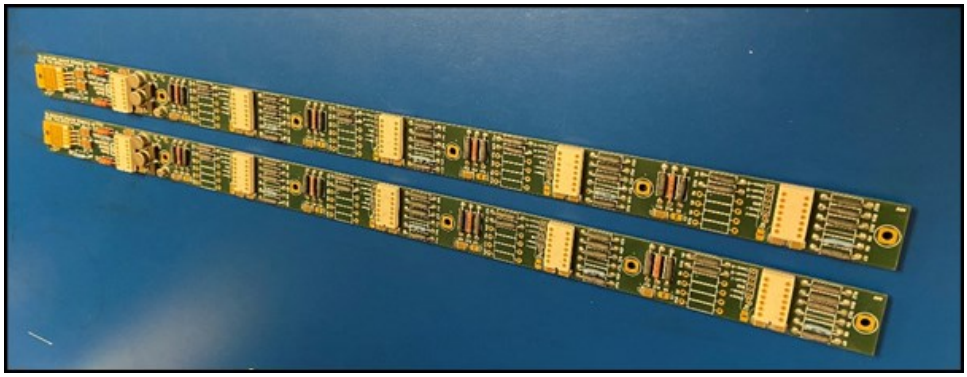

Figure 3: High-temperature Chemical Buffer Amplifier (CBA) for accommodating additional signal inputs.

In a parallel effort to capture and transmit data from the chemical sensors to the surface using commercial off-the shelf (COTS) components, Sandia is investigating the use of the EV-HT-200CDAQ1 High-Temperature Data Acquisition Reference Design Platform from Analog Devices as an alternative system microcontroller. This device, seen in Figure 4, is capable of interfacing with the CBA and the Mitco PTS module and uses an RS485 serial connection to transmit the data it gathers. The current effort has focused on developing software to operate the microcontroller with the high-temperature logging tool and confirming the rated operating temperature of 200 ˚C over several days of oven testing.

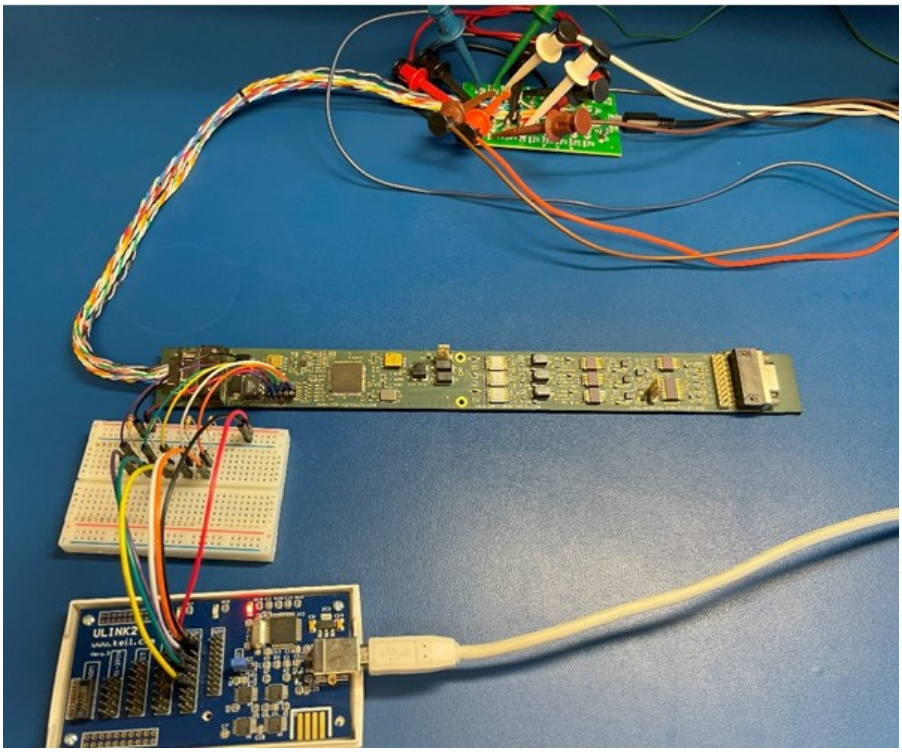

Figure 4: Alternative off-the-shelf system microcontroller - EV-HT-200CDAQ1 from Analog Devices.

The remaining tasks to get the board operable within the system are to confirm the operation of the RS 485 communication link through the wireline and to write the code necessary to interface with the Mitco PTC module.

2.1.2 Chemical Sensor Housing

Based on flow modeling results and integration considerations, a new sensor housing has been designed and developed to integrate with the existing logging tool (Figure 5), which is also referred to as tool housing version 2 in the numerical simulation work (see Section 3.2). The retainer has slots to incorporate three Ion-selective Electrode (ISE) sensors, one reference sensor, and two pH sensors. The chemical sensor was redesigned to incorporate a CuAg-plated pellet wire adapter to centralize the wire. The housing has a wire feed-thru to accommodate a downstream commercial PTS sensor. The fabricated version of the component is also shown in Figure 5. The unique feature combinations (internal tube, pellet slots) are enabled through metal additive manufacturing.

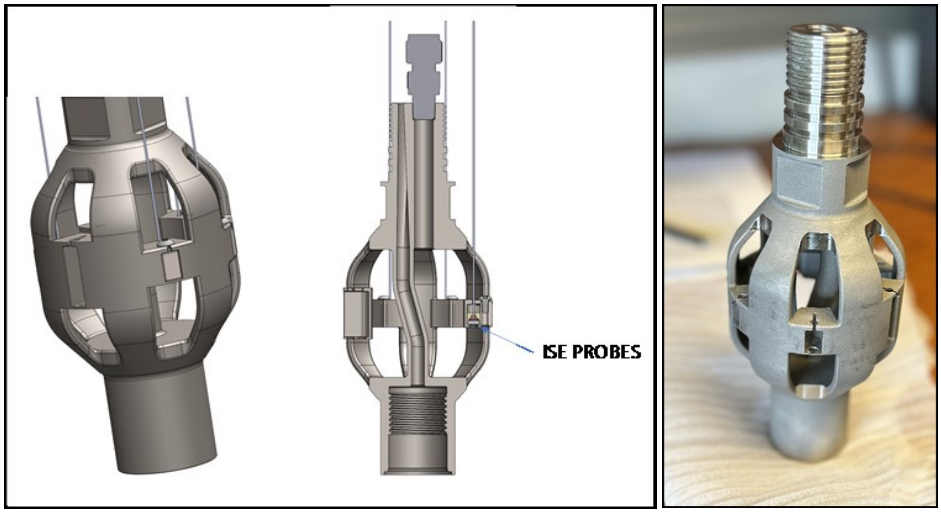

Figure 5: Sensor housing details (left) and fabricated sensor housing (right)

2.1.3 Tool Assembly

The final configuration of the overall tool is shown in Figure 6. The leading end of the tool will consist of a Mitco PTS sensor package to take secondary downhole measurements. That will adapt to the FORGE sensor package through the wire guide component. The sensor wires from both the ISEs and the Mitco PTS tool pass through to the electronics housing. The electronics housing connects to the wireline via a 7-conductor feedthrough.

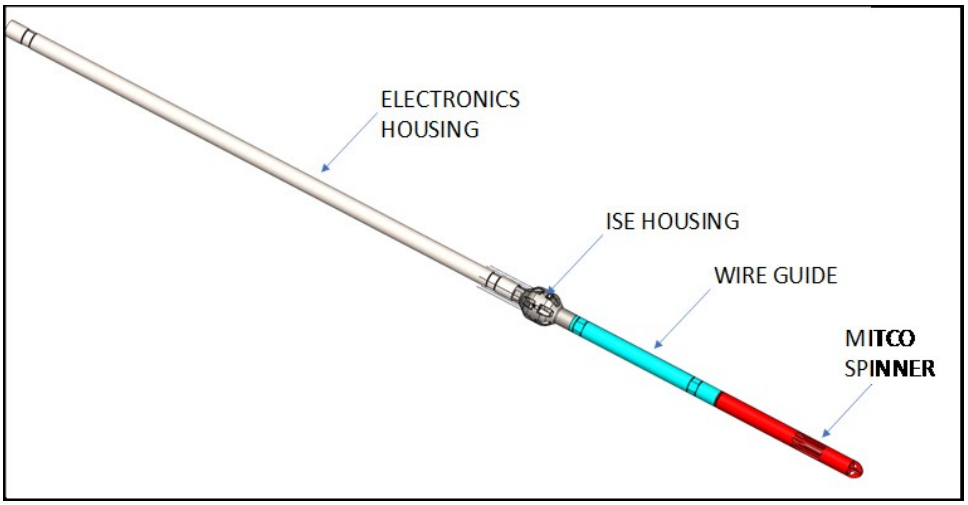

Figure 6: Overall tool assembly illustration

2.1.4 Deployment Plan

FORGE Wells 58-32 and Well 16B(78)-32 are being considered for deployment options. Well 58-32 is a vertical monitoring hole with a total depth of 9,105 ft. Well 16B(78)-32 was drilled vertically to a kick-off point of 5,269 ft with a curve built at 5°/ft and a 65° tangent to a total depth of 10,947 ft. The profiles for both wells are shown in Figure 7. A wireline truck will be used to deploy tool into the well. For 58-32, the weight of the tool will likely be sufficient to lower the tool with gravity; however, in 16B(78)-32, a wireline roller from Petromac can be used to help convey the tool through the curve. Table 1 provides an overview of the two FORGE wells and the deployment techniques in each.

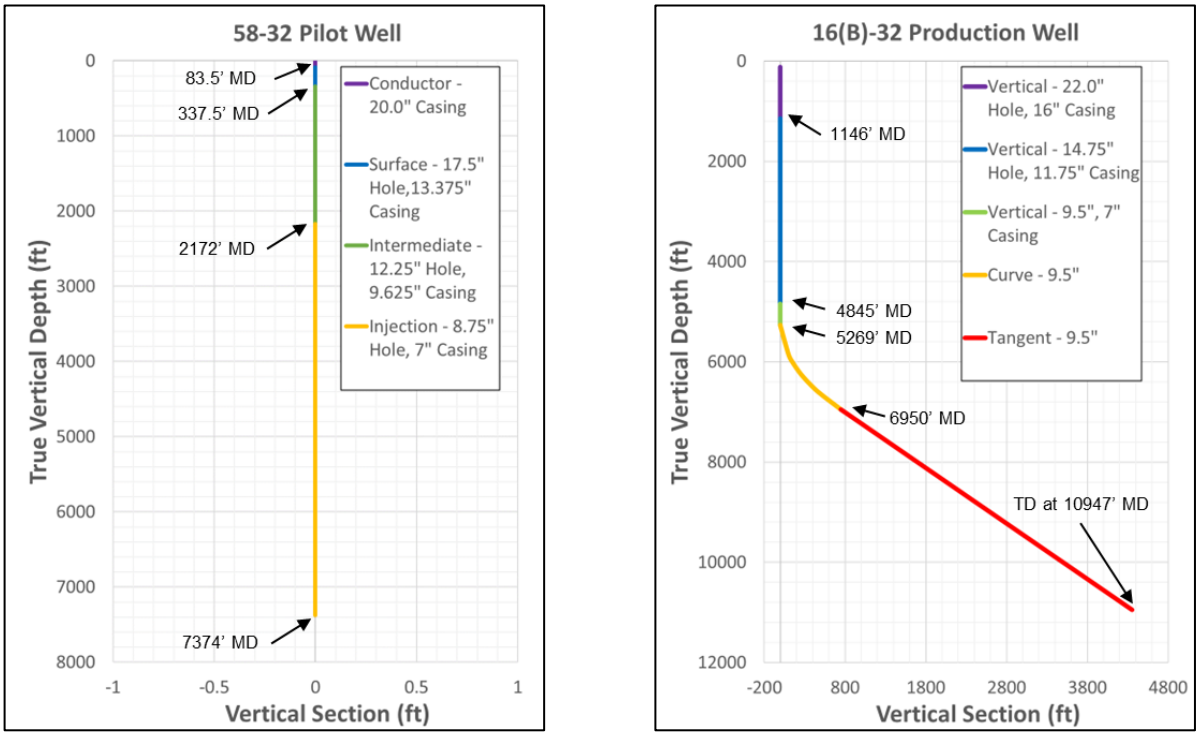

Figure 7: Utah FORGE Well 58-32 Profile (left) and Well 16B(78)-32 Profile (right).

Table 1: Overview of tool deployment scenarios in Utah FORGE wells 58-32 and 16B(78)-32.

FORGE Well	Well Type	Curve Profile	Total Depth	Deployment Technique
58-32	Vertical Pilot Well	N/A	7374 ft	Tool deployed on wireline with weight of tool
16B(78)-32	Directional Production Well	5°/100 ft	10,947 ft	Tool deployed on wireline with Petromac roller to assist with well deviation

3. UPDATES ON NUMERICAL SIMULATIONS

3.1 Simulations with Downhole Temperature and Pressure

Numerical simulations were previously conducted at the laboratory scale based on the artificial well system's dimensions at the Stanford Geothermal Laboratory and under ambient pressure and temperature conditions. To prepare for the upcoming field test, numerical simulations were initiated at the field scale. The same base case scenarios from the laboratory scale were used, but they were run under Utah FORGE temperature and pressure conditions, which are 225°C and 5000 psia, respectively. Two cases were run: one with the tool inside the wellbore and one without it, known as the undisturbed and disturbed state, respectively.

As shown in Figure 8, there was no substantial difference in fluid flow behavior between the pressure and temperature conditions encountered downhole and those at ambient conditions. This result is expected because the phase of the fluid remains in a liquid state despite the marked difference in temperature and pressure. Hence, the flow behavior should be similar to the laboratory-scale simulations, given that the wellbore dimension or inflow rate was kept the same.

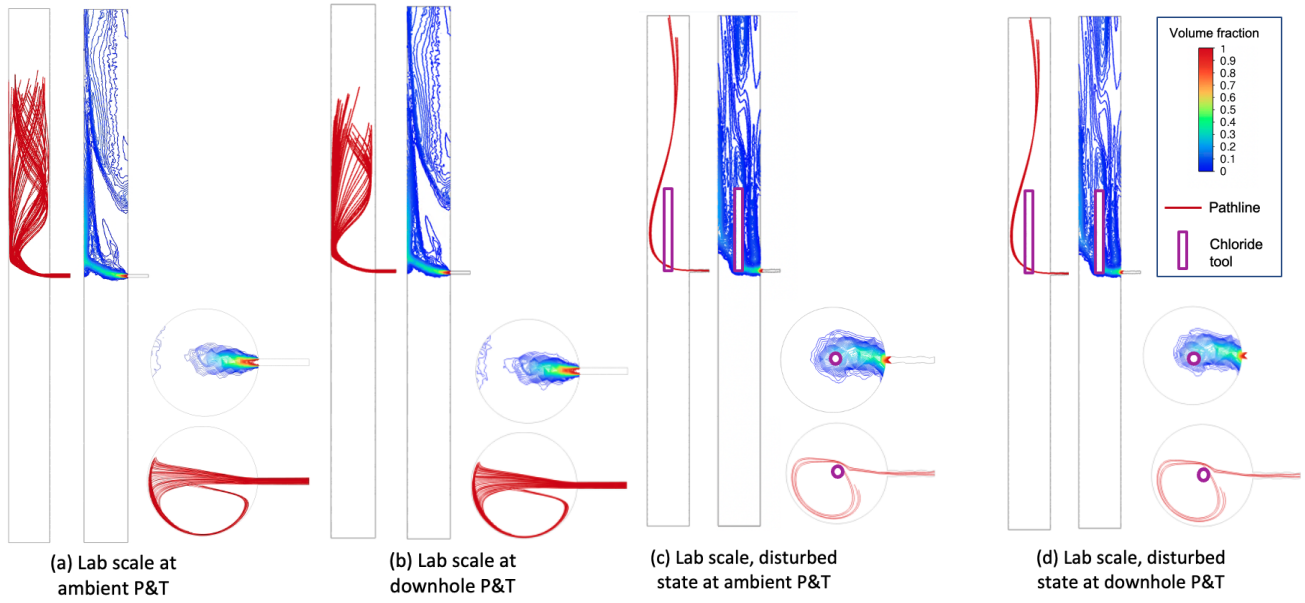

Figure 8: Comparison of the laboratory base cases of the undisturbed (a and b) and disturbed (c and d) states at laboratory ambient temperature versus at Utah FORGE downhole pressure and temperature.

3.2 Field-scale Tool Housing Simulations

Subsequent simulations were conducted involving version 1 of the field-scale tool housing, which had four pillars surrounding a centralized chloride ISE probe and allowed the lab-scale prototype to be plugged in. To ensure effective meshing and avoid excessive simulation time, the field tool design was simplified down to the essential shape that still affects flow behavior without the additional complexities involving nuts, bolts, and ridges. Figure 9 shows the simplified design.

The main issue to test for this design was the change in flow behavior when the feed zone encounters the pillars in the tool housing design, known as the obstructed flow case. This case needs to be avoided, as the obstruction would inhibit the feed zone inflow from reaching the ISE probes located at the center of the housing, resulting in flow rate underestimation. The ideal scenario for this design would be the free flow case, as the feed zone jet can reach the ISE probes at the center directly.

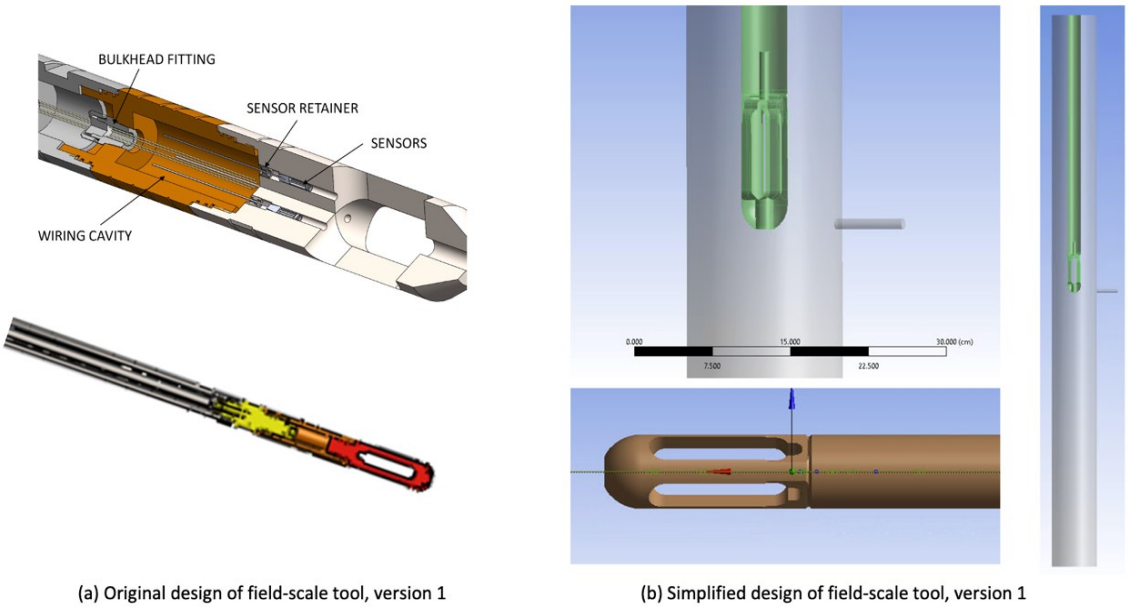

(a) Original design of field-scale tool, version 1

(b) Simplified design of field-scale tool, version 1

Figure 9: (a) original design of the field-scale tool, version 1, and (b) the simplified housing and tool dimension in preparation for numerical simulation cases

The results of the obstructed flow and free-flow cases are shown in Figure 10 and Figure 11, respectively. These figures display the progressive motion of the tool as it runs down the wellbore. It is important that sufficient chloride concentration reaches the middle crevice where the chloride tool will be situated.

In the obstructed case, it is observed that only a small chloride concentration, ranging from 0% to 0.2% of the original volume fraction, can reach the center of the housing. The highest chloride concentration that can reach the lower center of the housing is when the tip of the tool faces the feed zone. In this case, the concentration can reach around 50% of the original, as shown in Figure 10a. Meanwhile, the free-flow case (Figure 11c) shows that the inflow can easily reach the center while retaining a volume fraction of around 85%.

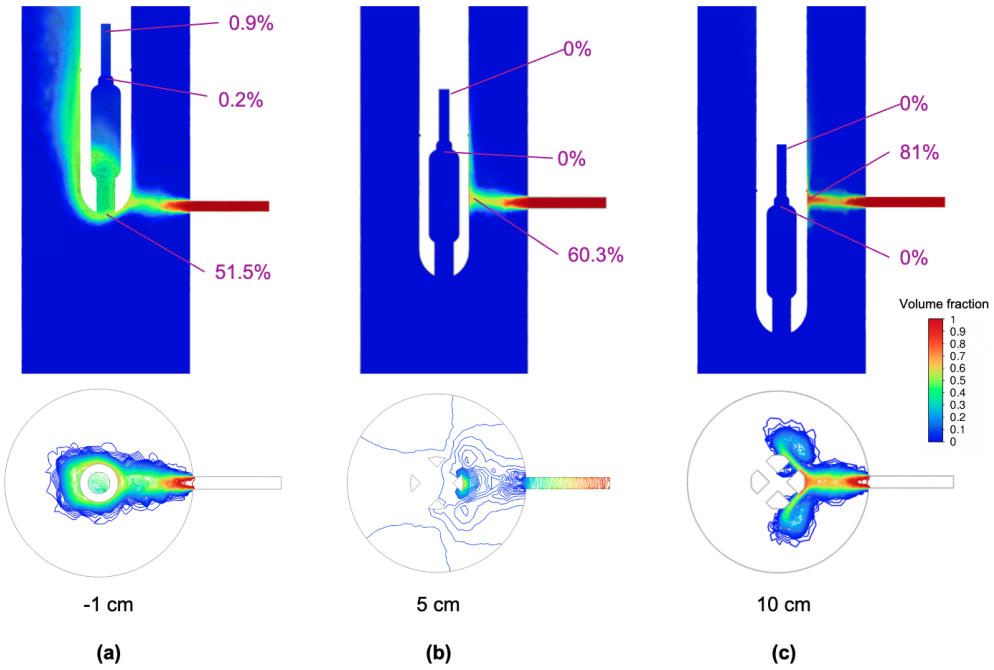

Figure 10: Simulation results of the unobstructed flow case of the field-scale tool version 1; (a, b, c) represent the progression of the tool housing penetrating through the wellbore at a certain offset of the feed zone height. The upper graphics show the vertical cross-section, while the lower graphics show the horizontal cross-section at feed zone height.

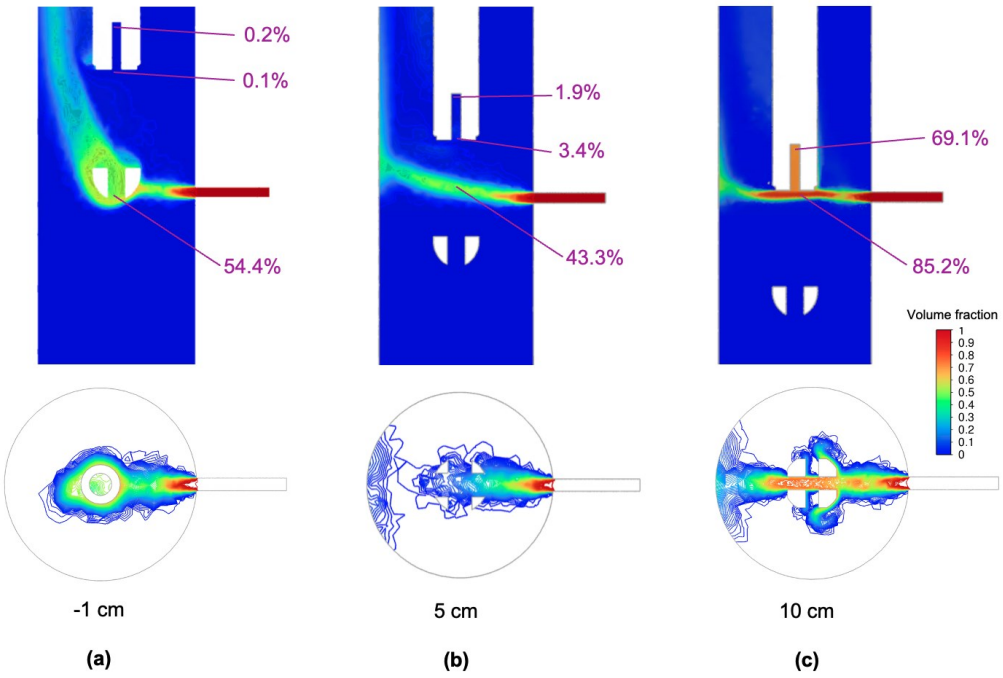

Figure 11: Simulation results of the free-flow flow case the field-scale tool version 1; (a, b, c) represent the progression of the tool housing penetrating through the wellbore at a certain offset of the feed zone height. The upper graphics show the vertical cross-section, while the lower graphics show the horizontal cross-section at feed zone height.

Version 2 of the field tool comes with a housing that has six pillars and a retainer placed at the edges. The retainer has slots to accommodate three ISE sensors, one reference sensor, and two pH sensors, which are shown in Figure 5. To conduct simulations, we used a simplified version of the housing, as illustrated in Figure 12.

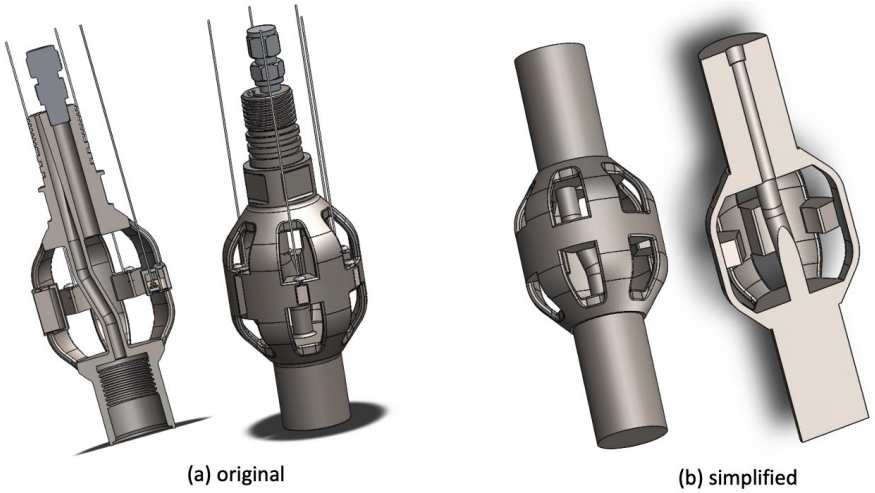

Figure 12: Simplified housing and tool dimension in preparation for numerical simulation cases for field tool housing version 2

The simulations for version 2 were similar to version 1, and they focused on the positioning of the ISE sensors in relation to the feed zone inflow. Five locations were tested and identified as positions *a* to *e* in Figure 13. These positions represent the relative location of the feed zone inflow and the tool body when it is inserted into the wellbore in the Run in Hole (RIH) motion. The number in cm shows the feed zone height offset relative to the center of the housing, ranging from 2.7 cm below the center (i.e., position *a* at -2.7 cm) to 2.7 cm above the center (i.e., position *b* at +2.7 cm).

The boundary conditions are kept the same with all the base cases and mimic the laboratory base case setup, i.e., two inlets and an outlet. The first inlet is from the feed zone at 112.2 ml/s, and the second inlet is from the bottom of the well at 2.09 kg/s representing the wellbore internal flow. Finally, the pressure outlet is at the top of the well, representing the wellhead. Two types of scenarios were tested for each position: when the feed zone inflow entered the crevice of the housing and when the feed zone inflow faced one of the pillars, which was

at a 30-degree angle from the center of the crevice. The case groups representing the two scenarios are called free-flowing and obstructed case groups, respectively, the same as simulations for version 1.

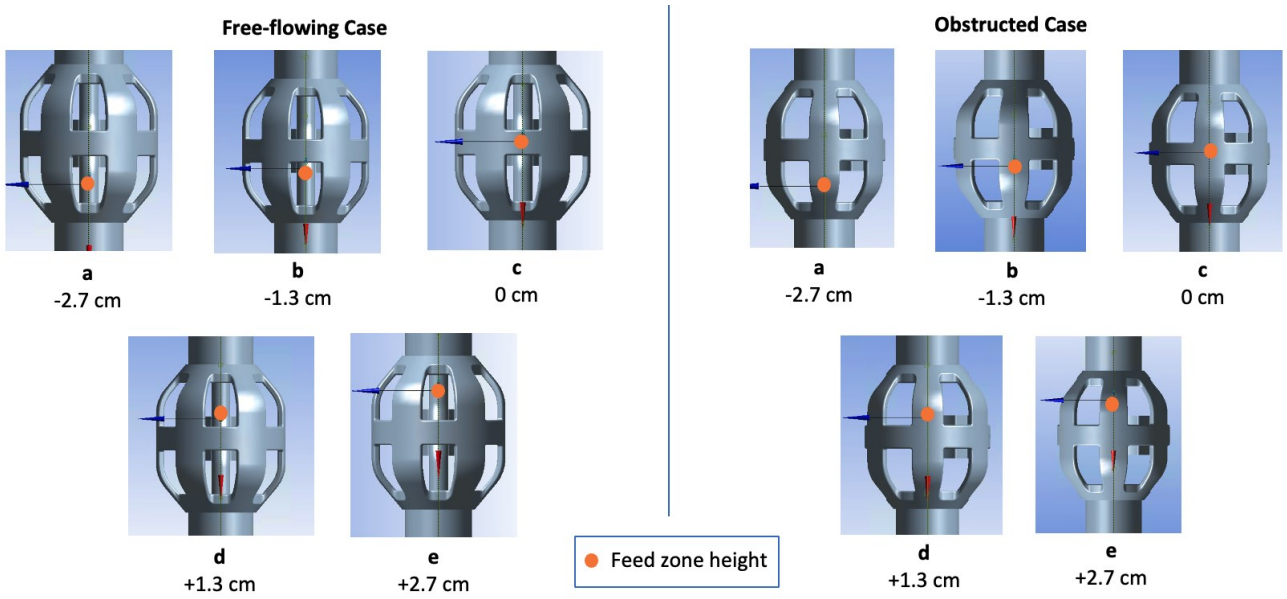

Figure 13: Five positions of the tool housing relative to the feed zone height labeled from a to e. Positions are chosen to represent the Ream in Hole (RIH) motion of the chloride tool. The number in cm shows the feed zone height offset relative to the center of the housing. Two case groups are simulated: the free-flowing case group (left), where the feed zone inflow faces the opening; the obstructed case group (right), where the feed zone inflow faces one of the pillars.

The modeling results are shown in Figure 14 as a horizontal cross-section and in Figure 15 as a vertical cross-section at sensor height, which is 1.4 cm below the center of the housing. The horizontal cross-section illustrates the inflow behavior in and around the housing as the tool progressed in RIH motion, while the vertical cross-section depicts the distribution around the tool sensor.

The free-flow case group allows the inflow to form a jet, passing through the housing. The ISE probe located right in front of the feed zone records the highest concentration at around 50-60%. The concentration disperses to 30-40% within the jet stream coverage. However, outside the jet stream coverage, the concentration drops significantly to 0-20% of the original volume fraction. Position *a* and *b,* achieved at the beginning of the tool reaming in, show the strongest and most uniformly distributed chloride concentration.

In the obstructed flow case group, the inflow jet is blocked by a pillar, which causes the fluid to be diverted around the perimeter. Figure 15 shows that the two nearest ISE probes on the right and left of the pillar will receive the highest concentration readings between 40% and 50%. The rest of the probes would receive almost no fluid. However, the most uniformly distributed chloride concentration is observed in position a, shown in Figure 15. The distribution is rather circular, encompassing all six sensor placements in the housing. Having the inflow jet facing the pillar allows the jet to be distributed around the perimeter of the housing, uniformly hitting all the sensors. Based on simulations at different positions and timing standpoints, it appears that the best signal will be recorded at the beginning of the RIH motion when the lower part of the housing meets the feed zone.

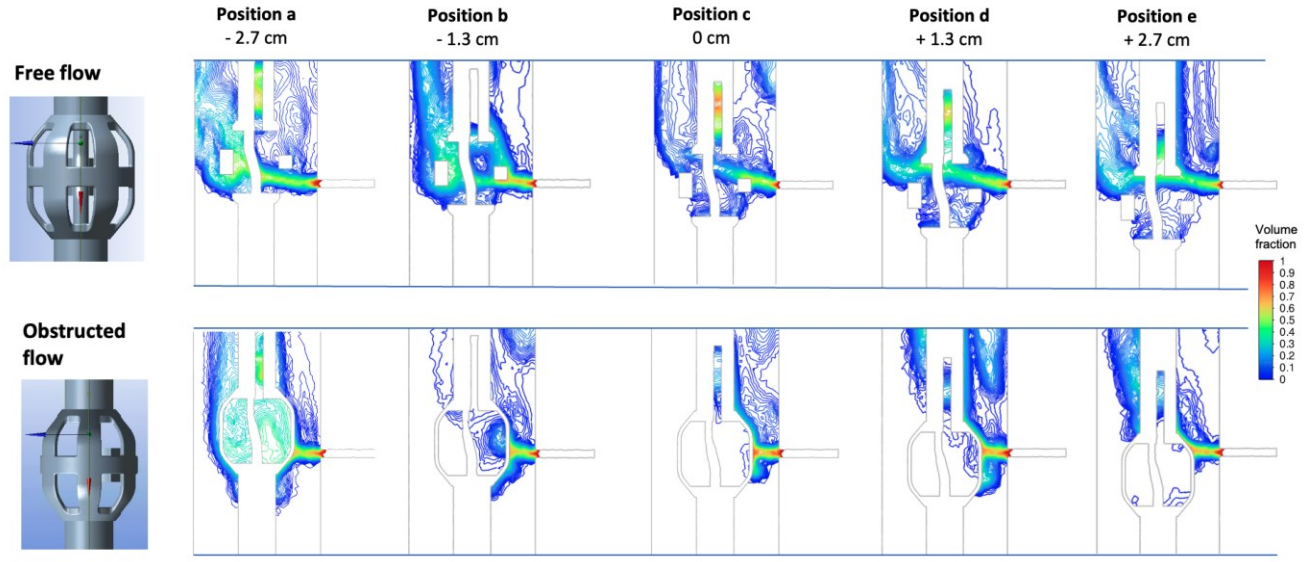

Figure 14: Modeling results are shown as vertical cross sections; the case group at the top represents the free-flow case, and the case group at the bottom represents the obstructed-flow case.

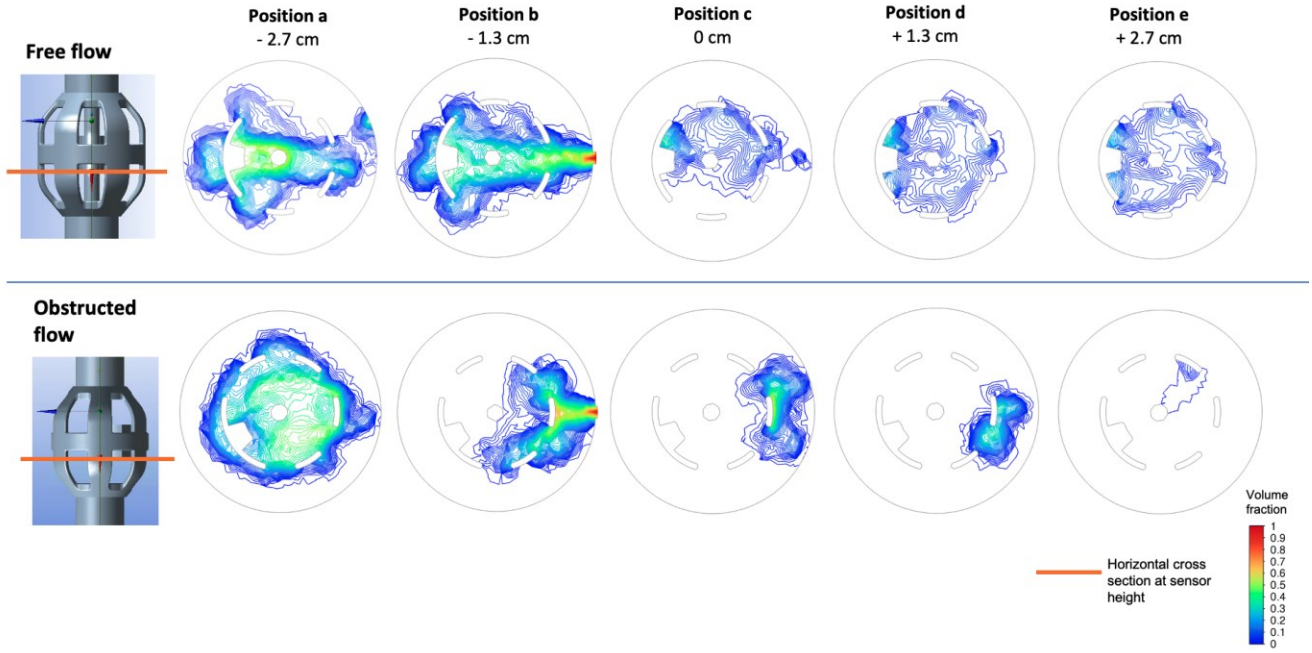

Figure 15: Modeling results are shown as horizontal cross sections at the sensor height, indicated by the orange line; the case group at the top represents the free-flow case, and the case group at the bottom represents the obstructed-flow case.

4. UPDATES ON LABORATORY EXPERIMENTS

In parallel with the numerical simulations and tool fabrication, the laboratory work investigated electromagnetic interference affecting the voltage signal reading and improved the tool running mechanism.

4.1. Signal Interference Reduction

In earlier experiments, we had experienced problems with electromagnetic noise affecting the voltage signals received at the data acquisition system. To address this problem, the electromagnetic fields (EMF) were tested around the equipment to identify the sources of the interference (see Figure 16a). An EMF meter was used. As a result of the investigation, several modifications to the laboratory setup were made, such as:

(a) Wrapping Faraday mesh around objects where a high EMF signal was detected, whenever possible, such as the reservoir inflow pump, power adapter, AC to DC power converters, data acquisition (DAQ) hardware, and cables (Figure 16b). However, some sources of interference could not be shielded with Faraday mesh due to safety reasons, such as the methane detectors nearby in the lab.
(b) Moving the DAQ tool and the computer to a greater distance from the artificial well system and onto the nearby bench to reduce the number of electronics devices situated around the chloride tool.
(c) Replacing the AC pump with a DC type.

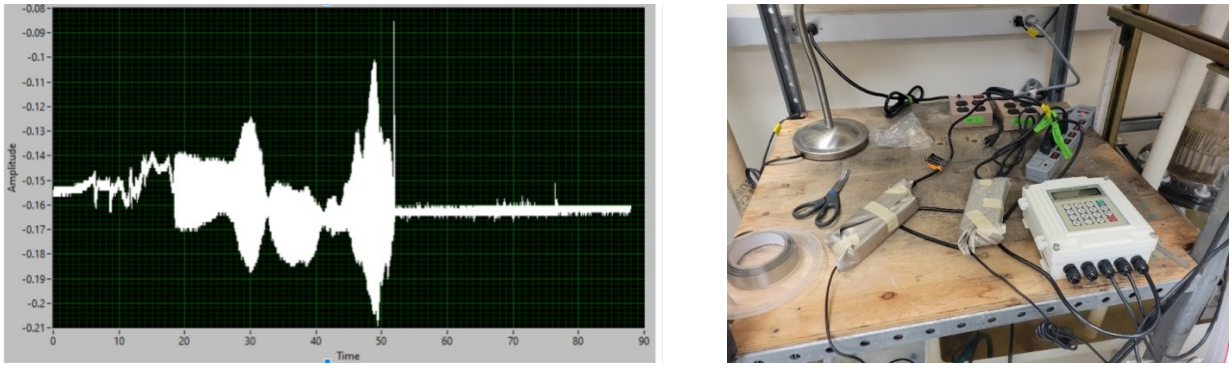

(a) (b)

Figure 16: (a) example of the EMF interference to the recorded voltage signal starting from time 20 seconds and ending at time 53 seconds (the start and stop times of the pump); (b) Faraday mesh applied to the AC to DC power converters.

The modifications yielded positive results in reducing the interference noise in the voltage data. Among the modifications, exchanging the AC pump with a DC one was the most effective in dampening interference. However, applying the Faraday mesh and relocating the computer and DAQ also helped. As a result of these modifications, the voltage signal has a smaller variation, similar to the signal recorded between time 0 to 20 seconds in Figure 16a. The increased fidelity of the signal indicates a successful reduction in EMF interference.

4.2. Tool Running Mechanism Modifications

Modifications and alterations were made to the running mechanism of the tool to improve its operation. The most notable change was the elimination of a dual electric connection and motion system. This redesign involved changing the driving mechanism of the running system to use the electric cable connected to the tool instead of using a single-strand wire. This change improved the stability and accuracy of placement due to the thicker diameter of the electric cable. Figure 17a shows the chloride tool with the electric cable attachment in the artificial wellbore.

Additionally, the routing mechanism to connect the chloride tool to the data acquisition (DAQ) hardware was also altered. Figure 17b shows the rerouted electric cable exiting the wellbore to connect with the digital acquisition hardware. Changes were made to this routing by adding pullies that can lower the friction associated with the movement of the cable and prevent entanglement with the well system's scaffolding.

(a) (b)

Figure 17: Modifications applied to the running mechanism to improve its operation: (a) updated driving mechanism, now using tool's electric cable to drive the movement in and out of the wellbore; (b) Updated routing of the electric cable connecting the chloride tool and the data acquisition (DAQ) hardware.

5. CONCLUSION

Updates on the chloride tool development focus on the development of the field-scale tool in anticipation of the field trial at the Utah FORGE site.

The field-scale tool fabrication has been underway, testing different iterations of the sensor pellet, tool housing, and assembly. Core components include a Honeywell microcontroller, Sandia's custom high-temperature ASIC, and Mitco's PTS module. Data is transmitted to the surface through Frequency Shift Keying (FSK) and a multiconductor wireline. A high-temperature Chemical Buffer Amplifier (CBA) board was developed for signal conversion and amplification of the chemical sensors, operating at temperatures up to 260°C. Additionally, an alternative system microcontroller from Analog Devices is being explored for data transmission at 200°C. Furthermore, a new sensor housing, fabricated using metal additive manufacturing, was designed to integrate with the logging tool, accommodating Ion-selective Electrode (ISE) sensors, reference sensors, and pH sensors. The tool assembly features a Mitco PTS sensor package, a wire guide component, and electronics housing for data transmission through a 7-conductor feedthrough to the wireline.

The tool is planned to be deployed at FORGE Wells 58-32 (vertical well) and Well 16B(78)-32 (deviated well). For 58-32, the weight of the tool will likely be sufficient to lower the tool with gravity; however, in 16B(78)-32, a wireline roller can be used to help convey the tool through the curve.

Numerical simulations were also conducted at the field scale. Firstly, simulation base cases were modified to include the downhole conditions of 225°C and 5000 psia. Two primary scenarios were examined: one with the tool inside the wellbore (disturbed state) and one without it (undisturbed state). Surprisingly, the simulations showed that despite the significant differences in temperature and pressure, there was no substantial alteration in fluid flow behavior between the laboratory and field conditions. This similarity was attributed to the fluid remaining in a liquid state.

Further simulations focused on the design of the field-scale tool housing. The objective was to understand how the housing affected flow behavior when encountering the feed zone. Version 2 of the field tool featured six pillars and sensor slots located at the axial perimeter of the housing rather than centralized in the middle of the housing. Version 2 of the housing is the one fabricated for the tool assembly. For Version 2, five positions were tested, each representing a relative offset of the feed zone height. Additionally, each position was used twice: in free-flow and obstructed case groups. In the free-flow case, inflow formed a jet, resulting in higher chloride concentrations at specific sensor locations. In contrast, the obstructed flow case saw the inflow diverted around pillars, leading to more uniform chloride distribution among the sensors. The simulations suggested that the best signal recordings occurred at the beginning of the tool's Run in Hole (RIH) motion when the lower part of the housing met the feed zone.

In parallel with the field-scale tool fabrication and numerical simulation, the laboratory work focused on addressing the EMF noise affecting the voltage readings , as well as reconfiguring the tool positing system system. Modifications were made to the equipment to curb EMF interference, which included replacing the AC pumps with DC type, having EMF-emitting electronics wrapped with Faraday mesh whenever possible, and relocating possible interference sources away from the sensors. The modifications have been successful in curbing the interference issue.

Additional modifications to the tool positioning system were implemented to eliminate the dual electric connection and motion system. The stability of the laboratory-scale chloride tool movement was improved by modifying the driving mechanism. The friction was lowered by altering the cable routing between the chloride tool and the DAQ hardware. This redesign allows for increased stability of the driving mechanism and improved efficiency.

ACKNOWLEDGMENTS

This work is part of the Utah FORGE project under award number 3-2418 as a collaborative project between Stanford University and Sandia National Laboratory, supported by the U.S. Department of Energy. Sandia National Laboratories is a multimission laboratory managed and operated by National Technology & Engineering Solutions of Sandia, LLC, a wholly-owned subsidiary of Honeywell International Inc., for the U.S. Department of Energy's National Nuclear Security Administration under contract DE-NA0003525. This paper describes objective technical results and analysis. Any subjective views or opinions that might be expressed in the paper do not necessarily represent the views of the U.S. Department of Energy or the United States Government. Paper registration ID: SAND2024-01075C.

REFERENCES

Acuña, J. A. and. Arcedera B. A.: Two-Phase Flow Behavior and Spinner Data Analysis in Geothermal Wells, Proceedings 13th Workshop on Geothermal Reservoir Engineering, Stanford University, Stanford, California (2005).

Sullivan, J.L., Clark, C.E., Han, J., Wang, M.: Life-Cycle Analysis Results of Geothermal Systems in Comparison to Other Power Systems, Argonne National Laboratory ANL/ESD/10-5 (2010)

Fei, F., Lu, Y., Bunger, A. P., & Cusini, M.: Experimental and Numerical Study of Hydraulic Fracturing in Enhanced Geothermal Systems (EGS), Proceedings 48th Workshop on Geothermal Reservoir Engineering, Stanford University, Stanford, California (2023).

Gao, X., Egan, S., Corbin, W.C., Hess, R.F., Cieslewski, G., Cashion, A.T., and Horne, R.N.: Analytical and Experimental Study of Measuring Enthalpy in Geothermal Reservoirs with a Downhole Tool, GRC Transactions, Vol.41(2017).

Huenges, E.: 25 - Enhanced geothermal systems: Review and status of research and development, Geothermal Power Generation, Woodhead Publishing, Pages 743-761, (2016).

Judawisastra, L. H., Sausan, S., Cherng-Su, J., Horne, R. N.: Development Update on Chloride-based Inflow Measurement in Fractured Enhanced Geothermal Systems (EGS) Wells, Proceedings 48th Workshop on Geothermal Reservoir Engineering, Stanford University, Stanford, California (2023).

Judawisastra, L. H., Sausan, S., Horne, R. N.: Analytical, Experimental and Numerical Development Update on Inflow Measurement in Geothermal Wells from Chloride Concentration. Proceedings, 8th Indonesia International Geothermal Convention & Exhibition, (2022).

Sausan, S., Judawisastra, L. H., Horne, R. N.: Development of Downhole Measurement to Detect Inflow in Fractured Enhanced Geothermal Systems (EGS) Wells, Proceedings 47th Workshop on Geothermal Reservoir Engineering, Stanford University, Stanford, California (2022).

Sausan, S., Judawisastra, L. H., Cherng-Su, J., Horne, R. N.: Chloride-based Wireline Tool for Measuring Feed Zone Inflow in Enhanced Geothermal Systems (EGS) Wells: Experimental, Numerical, and Data-driven Updates, Geothermal Resources Committee Transactions Vol 47 (2023), pg. 841-863.

Sausan, Sarah: Investigating Fluid Flow Behavior in Enhanced Geothermal System (EGS) Wells: Numerical and Data-Driven Approaches, MS Thesis, Energy Resources Engineering Department, Stanford University (2023).

Sisler, J., Zarrouk, S. J., Adams, R.: Improving the Performance of Geothermal Pressure, Temperature and Spinner (PTS) Tools Used in Down-Hole Measurements. Proceedings, World Geothermal Congress 2015, Melbourne, Australia (2015).